J. Fluid Mech. (1971), *vol.* 46, *part* 4, *pp.* 657–684
Printed in Great Britain

Three-dimensional MHD duct flows with strong transverse magnetic fields. Part 2. Variable-area rectangular ducts with conducting sides

By J. S. WALKER, G. S. S. LUDFORD
Department of Theoretical and Applied Mechanics, Cornell University
AND J. C. R. HUNT
Department of Applied Mathematics and Theoretical Physics, Cambridge University

(Received 23 July 1970)

In this paper the general analysis, developed in part 1, of three-dimensional duct flows subject to a strong transverse magnetic field is used to examine the flow in diverging ducts of rectangular cross-section. It is found that, with the magnetic field parallel to one pair of the sides, the essential problem is the analysis of the boundary layers on these (side) walls. Assuming that they are highly conducting and that those perpendicular to the magnetic field are non-conducting, the flow is found to have some interesting properties: if the top and bottom walls diverge, the side walls remaining parallel, then an $O(1)$ velocity overshoot occurs in the side-wall boundary layers; but if the top and bottom walls remain parallel, the side walls diverging, these boundary layers have conventional velocity profiles. The most interesting flows occur when both pairs of walls diverge, when it is found that large, $O(M^{\frac{1}{2}})$, velocities occur in the side-wall boundary layers, either in the direction of the mean flow or in the reverse direction, depending on the geometry of the duct and the external electric circuit!

The mathematical analysis involves the solution of a formidable integral equation which, however, does have analytic solutions for some special types of duct.

1. Introduction

In part 1, Hunt & Ludford (1968) embarked upon a general analysis of three-dimensional duct flows subject to a transverse magnetic field sufficiently strong for inertial effects to be negligible. The flow can then be divided into an inviscid core region, Hartmann boundary layers on walls intersecting the magnetic field, and narrow viscous regions parallel to the magnetic field. These can either be boundary layers on the walls or free shear layers within the fluid emanating from obstacles in the flow or discontinuities at the duct walls. Apart from setting up the machinery for treating such flows in general, in which it was found that the core flow is largely determined by a new three-dimensional jump condition across the Hartmann layers, the emphasis of part 1 was on analysing flows over obstacles in channels of constant area. [No direct mention of the side walls was

made because they only modify the flow near the obstacle in an inessential way, at least for insulating or conducting walls on open circuit, cf. §8.]

After publication of part 1 it was discovered that Kulikovskii (1968) had already derived some of this general analysis. However, the emphasis of his work is less physical and he does not treat the problem mentioned above. Also, since publication of part 1, the theory has been confirmed, with unjustifiable accuracy, from experiments measuring the drag on a sphere placed in a transverse magnetic field. Further discussion is given in §2 and by Hunt (1970).

Part 1 ended with a promise to apply the general theory to ducts of varying cross-section (hereafter called diverging), and the present paper is a first step in this direction. We shall concentrate on the most practical class, namely symmetric rectangular ducts whose side walls (parallel to the applied magnetic field) are perfect conductors, the other two walls being insulators (see figure 1). [Clearly other combinations of wall conductivity will produce as varied flows as they do in constant-area rectangular ducts.] The essential problem is to determine the boundary layers on the side walls. Fortunately the completely local character of these side layers makes their analysis tractable.

The first type of duct considered (§2) has parallel side walls, this being the situation envisaged by Hunt & Leibovich (1967) in their two-dimensional treatment of diverging channels. They assumed that satisfactory side layers could be constructed for their core flow, and one of our objectives is to prove this. A first glance suggests a straightforward modification of the structure of the side layers in constant-area ducts found by Hunt & Stewartson (1965) and Chiang & Lundgren (1967). But the analysis shows otherwise. The governing integral equation (§3), which must in general be solved numerically (§4), normally leads to a velocity profile containing an overshoot which ensures zero flux deficiency in the layer. Correspondingly, there is no first-order disturbance of the core flow. It is shown in §5 that the constant-area results are basically correct only when the divergence of the duct is small (at most comparable to the inverse square root of the Hartmann number). As the divergence tends to zero the velocity overshoot moves out into the core as a first-order perturbation, leaving behind a flux deficiency in the layer. Also in §5 an exact solution of the integral equation is obtained for a particular divergence.

In §6 we examine the more interesting type of duct whose side walls also diverge. That the flow is radically different can be seen from the general result found in part 1, §3, concerning current lines in the core. For rectangular ducts these lines lie in the cross-sections and are parallel to the non-conducting walls (so long as the latter are diverging). When the side walls are perpendicular to these current lines, as in §2, there is no violation of the boundary condition at a perfect conductor, namely zero tangential current. The side layers need only accomodate the jump in tangential velocity. But when the side walls diverge there is also a tangential current to be reduced to zero, which entails a jump in electric potential across the layer. Such a jump† induces large velocities, in this case of the order of the square root of the Hartmann number. Thus the side layers are able

† This effect appeared in the free shear layer of part 1 and flows treated by Moffatt (1964) and Hunt (1965).

to carry a substantial part of the total flux through the duct. In some cases there is even an excess flux through the core and a reverse flux through these layers; for instance, when both pairs of walls are diverging and the side walls are shorted. The analysis of §6 follows that in §§2–5, with another integral equation to be solved by similar methods.

The exceptional case where the top and bottom walls are parallel is considered in §7. In this type of duct the current lines are no longer confined to cross-sections, being determined by a solution of Laplace's equation, as shown in part 1. The current lines in the core can once again approach the side walls normally so that no potential jump is required across the side layers. In fact, these layers are locally of the kind found in constant-area ducts.

A discussion of the three types of ducts is given in §8, and in particular their roles as parts of a general symmetric duct. A duct with both pairs of walls diverging exponentially is used to illustrate the division of flux between the core and side layers in the second type (§6). Finally a simple example shows how our analysis can be easily adapted to non-symmetric ducts.

A fuller treatment is given in Walker's (1970) thesis.

2. Formulation of the problem for parallel side walls

When the magnetic Reynolds number $R_m = \mu U_0 \sigma d$ is small, the equations governing the steady flow of an electrically conducting liquid of uniform properties under the action of a transverse magnetic field, $\mathbf{B}_0$, are, in non-dimensional form,

$$(\mathbf{v}.\nabla)\mathbf{v} = -\nabla p + N(\mathbf{j}\times\hat{\mathbf{y}}) + R^{-1}\nabla^2\mathbf{v}, \tag{1a}$$

$$\mathbf{j} = \nabla\phi + \mathbf{v}\times\hat{\mathbf{y}}, \tag{1b}$$

$$\nabla.\mathbf{j} = 0, \quad \nabla.\mathbf{v} = 0, \tag{1c,d}$$

as used in part 1. (For their derivation see Hunt & Leibovich (1967).) Here

$$N = \sigma B_0^2 d/\rho U_0 \quad \text{and} \quad R = \rho U_0 d/\eta$$

are the interaction and Reynolds numbers, respectively, while $\hat{\mathbf{y}}$ is the unit vector in the direction of $\mathbf{B}_0$.

The present duct (shown in figure 1) has parallel plane side walls so that half their distance apart will be taken for the characteristic length d. The average velocity at some section, say $x = 0$ with the x axis along the centreline of the duct, will be used for the characteristic velocity U_0. Thus

$$\int_{-1}^{+1}\int_{-f(0)}^{+f(0)} u(0,y,z)\,dy\,dz = 4f(0). \tag{2}$$

As boundary conditions we have

$$\mathbf{v} = 0, \quad j_y = \pm f'(x) j_x \quad \text{at the insulating walls} \quad y = \pm f(x), \tag{3a}$$

and

$$\mathbf{v} = 0, \quad j_x = j_y = 0 \quad \text{at the perfectly conducting walls} \quad z = \pm 1. \tag{3b}$$

Together with the governing equations (1) these form a homogeneous problem whose solution is normalized by the condition (2). Since the pressure p and the

electric potential ϕ do not appear in any of the conditions (2), (3), it is convenient to eliminate them from the system (1) to obtain

$$N^{-1}\nabla\times[(\mathbf{v}.\nabla)\mathbf{v}] = \partial\mathbf{j}/\partial y + M^{-2}\nabla^2(\nabla\times\mathbf{v}), \tag{4a}$$

$$\nabla\times\mathbf{j} = \partial\mathbf{v}/\partial y, \quad \nabla.\mathbf{j} = 0, \quad \nabla.\mathbf{v} = 0 \tag{4b,c,d}$$

for the velocity $\mathbf{v}$ and current $\mathbf{j}$ alone. Having determined the latter p and ϕ follow from equations (1a, b). Here

$$M = N^{\frac{1}{2}}R^{\frac{1}{2}} = B_0 d(\sigma/\eta)^{\frac{1}{2}}$$

is the Hartmann number.

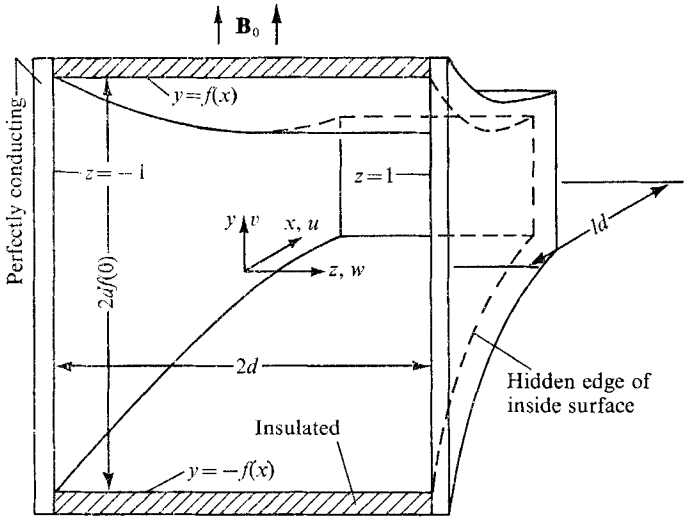

FIGURE 1. Duct with parallel side walls.

The only assumption so far is

$$R_m \ll 1; \tag{5a}$$

now we take in addition

$$N, M \gg 1. \tag{5b}$$

These three conditions can be satisfied in various ways, and do not necessarily imply that the Reynolds number R is large. For example, a small σ but large σB_0^2 leaves R arbitrary; on the other hand, small U_0 and large B_0 will give $R \ll 1$. We stress this because part 1 gives the impression that the analysis is *only* valid if $R \gg 1$. However the intention was to indicate that inertial terms can be ignored *even if* $R \gg 1$, provided M is large enough, such being the necessary experimental conditions if accurate measurements of velocity are to be made. In fact, in the experiments of Kalis, Slyusarev, Tsinober & Shtern (1966), on the drag of bluff bodies placed in a duct flow, R was not particularly large (about 20). In these Riga experiments N was about 2500 so that the condition $N \gg R^3$ for the part 1 theory to be valid was not grossly violated. Nevertheless, this does not explain why a theory considered unrealistic by Hunt & Ludford themselves is in such good agreement (Hunt 1970) with experimental results. But this agreement does suggest that similar experiments should also compare well with the theory of part 2.

Under the conditions (5), the flow region may be divided into separate parts, certain terms being neglected in each subregion. A central core is surrounded by thin layers in the fluid adjacent to the duct walls. If the divergence of the duct is smooth, all derivatives in the core are $O(1)$. The flux condition (2) indicates an $O(1)$ core velocity, and Ohm's law (1*b*) indicates an $O(1)$ current. Then the $O(N^{-1})$ inertia terms and the $O(M^{-2})$ viscous terms may be neglected, so that the momentum equation reduces to a balance between the Lorentz force and the $O(N)$ pressure gradient. The core solution does not, however, satisfy the conditions at the walls.

The solutions in the boundary layers must satisfy the wall conditions and match the core solution. Since they are very different for different duct geometries, we cannot assess the order of magnitude of the inertial terms at this stage. We shall assume N is large enough for the flow to be entirely inertialess, so that the layers required to satisfy $u = v = 0$ on the walls are the result of a viscous–electromagnetic balance. The assessment will be given in §8.

In part 2 we shall not be analysing the free shear layers within the fluid, where inertial effects can always be important. For example, such layers stem from sharp divergences in the duct walls (Hunt & Leibovich 1967) and from the edges of obstacles placed in the duct (part 1).

Without the inertia term, equation (4*a*) becomes

$$0 = \partial \mathbf{j}/\partial y + M^{-2}\nabla^2(\nabla \times \mathbf{v}), \tag{4a'}$$

and equation (1*a*) becomes

$$\nabla h = \mathbf{j} \times \hat{\mathbf{y}} + M^{-2}\nabla^2 \mathbf{v}, \quad \text{where} \quad h = N^{-1}p,$$

so that the Hartmann number is the only parameter left in the problem. The various subregions are shown in figure 2 (cf. Hunt & Stewartson 1965). (*a*) Core. All dimensions and derivatives are $O(1)$. (*b*) Hartmann boundary layers adjacent to the core of thickness $O(M^{-1})$, so that $\partial/\partial n = O(M)$ while $\partial/\partial s = O(1) = \partial/\partial t$. (*c*) Side-wall boundary layers of thickness $O(M^{-\frac{1}{2}})$, so that $\partial/\partial z = O(M^{\frac{1}{2}})$ while $\partial/\partial x = O(1) = \partial/\partial y$. The different structure of these layers from that of a

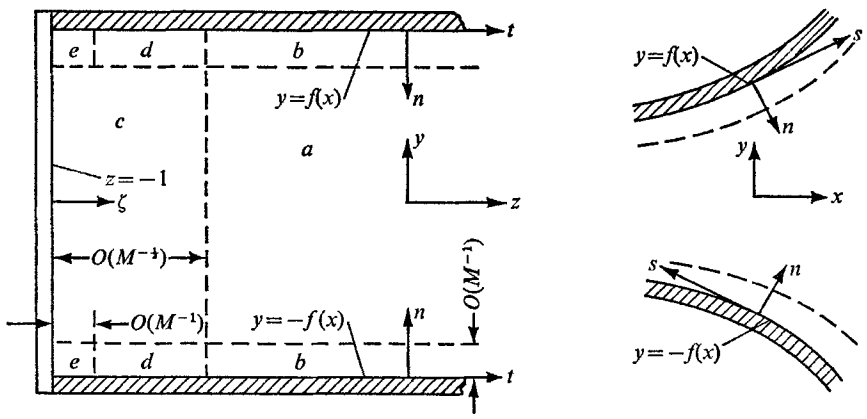

FIGURE 2. x and z sections showing subregions and notation.

Hartmann layer is due to the absence of a normal component of magnetic field. (*d*) Hartmann boundary layers adjacent to the side-wall layers of thickness $O(M^{-1})$ and breadth $O(M^{-\frac{1}{2}})$ in the z (or t) direction, so that $\partial/\partial n = O(M)$, $\partial/\partial t = O(M^{\frac{1}{2}})$, and $\partial/\partial s = O(1)$. These layers are still vanishingly thin on the scale of the side-wall layers. (*e*) Singular corner regions of dimensions $O(M^{-1})$ in an s = constant section, so that $\partial/\partial n = O(M) = \partial/\partial t$ while $\partial/\partial s = O(1)$. A side-wall layer will see a corner region as a point where values needed to match the adjacent Hartmann layer may not agree with those on the side-wall surface.

Expansions in M may be used to determine the flow in each region. First, the co-ordinates within a region are rescaled so that all derivatives are $O(1)$. The variables $\mathbf{v}, h, \mathbf{j}$ and ϕ are tentatively expanded as power series in $M^{-\frac{1}{2}}$, such as

$$u = u^{(0)} + u^{(\frac{1}{2})}M^{-\frac{1}{2}} + O(M^{-1}), \tag{6}$$

where the coefficients $u^{(i)}$ are functions of the (possibly scaled) co-ordinates alone. Powers of $M^{-\frac{1}{2}}$ are used because this is the largest parameter appearing in the equations and subregion dimensions.

Consider the solution in the core and adjacent Hartmann layers. The core variables, denoted by capital letters, satisfy

$$\partial \mathbf{J}^{(i)}/\partial y = 0, \quad \partial \mathbf{V}^{(i)}/\partial y = \boldsymbol{\nabla} \times \mathbf{J}^{(i)},$$
$$\boldsymbol{\nabla}.\mathbf{J}^{(i)} = \boldsymbol{\nabla}.\mathbf{V}^{(i)} = 0, \tag{7}$$

where

$$i = 0 \quad \text{or} \quad \tfrac{1}{2}.$$

The variables in the Hartmann layers are determined locally from the tangential velocity and current outside, and match the core variables provided the latter satisfy certain boundary conditions, which physically express continuity of velocity and current within the layer. Part 1 gives these conditions for a general insulator:

$$V_n = M^{-1}|\hat{\mathbf{n}}.\hat{\mathbf{y}}|^{-1}(\partial V_s/\partial s + \partial V_t/\partial t), \tag{8a}$$

$$J_n = M^{-1}\operatorname{sgn}(\hat{\mathbf{n}}.\hat{\mathbf{y}})\,(\partial V_t/\partial s - \partial V_s/\partial t), \tag{8b}$$

where (n, s, t) is a local right-handed co-ordinate system (see figure 2). In our case, these conditions become

$$f'U^{(i)} \mp V^{(i)} = 0, \quad f'J_x^{(i)} \mp J_y^{(i)} = 0 \quad \text{at} \quad y = \pm f(x). \tag{9a,b}$$

Provided the duct is actually diverging, i.e. $f'(x) \neq 0$, the general solution to (7) and (9) is

$$U^{(i)} = f(f')^{-1}d^2h^{(i)}/dx^2, \quad V^{(i)} = y\,d^2h^{(i)}/dx^2, \quad W^{(i)} = \partial\Phi^{(i)}/\partial x,$$
$$J_x^{(i)} = J_y^{(i)} = 0, \quad J_z^{(i)} = -dh^{(i)}/dx, \tag{10}$$

with the electric potential given by

$$\Phi^{(i)} = \psi^{(i)} - z(f')^{-1}\,d(f dh^{(i)}/dx)/dx, \tag{10'}$$

where $h^{(i)}(x)$ and $\psi^{(i)}(x)$ are integration functions representing the pressure and centreline potential. Note that these formulas can be taken to the limit $f' \to 0$

since the $d^2h^{(i)}/dx^2$ vanish like f', as we shall see later. They then give the constant-area duct solution.

In the side-wall layers, the z co-ordinate must be stretched locally. Near $z = \pm 1$, the substitution $\zeta = M^{\frac{1}{2}}(z \mp 1)$ gives a semi-infinite region with a side wall at $\zeta = 0$. The equations $(4a', b, c, d)$ to be solved are

$$\partial j_x^{(0)}/\partial y = \partial j_y^{(0)}/\partial y = \partial \mathbf{j}^{(0)}/\partial \zeta = \partial w^{(0)}/\partial \zeta = 0, \tag{11a}$$

and

$$\left.\begin{aligned} \partial j_x^{(\frac{1}{2})}/\partial y &= \partial^3 v^{(0)}/\partial \zeta^3, & \partial j_x^{(\frac{1}{2})}/\partial \zeta &= \partial j_z^{(0)}/\partial x + \partial v^{(0)}/\partial y, \\ \partial j_y^{(\frac{1}{2})}/\partial y &= -\partial^3 u^{(0)}/\partial \zeta^3, & \partial j_y^{(\frac{1}{2})}/\partial \zeta &= \partial j_z^{(0)}/\partial y - \partial u^{(0)}/\partial y, \\ \partial j_z^{(\frac{1}{2})}/\partial \zeta &= -\partial j_x^{(0)}/\partial x - \partial j_y^{(0)}/\partial y, & \partial w^{(\frac{1}{2})}/\partial \zeta &= -\partial u^{(0)}/\partial x - \partial v^{(0)}/\partial y. \end{aligned}\right\} \tag{11b}$$

The remaining pair of equations relate variables which are completely defined by these six equations and their boundary conditions. This redundancy was introduced by eliminating p and ϕ from (1) without appropriately reducing the number of equations.

The conditions (3b) for a perfectly conducting wall become

$$\mathbf{v}^{(i)} = 0 \quad \text{and} \quad j_x^{(i)} = j_y^{(i)} = 0 \quad \text{at} \quad \zeta = 0.$$

The Hartmann conditions (8) apply also in the side layers, where they yield

$$\left.\begin{aligned} f'u^{(0)} \mp v^{(0)} &= f' j_x^{(0)} \mp j_y^{(0)} = 0 \\ f' j_x^{(\frac{1}{2})} \mp j_y^{(\frac{1}{2})} &= \partial u^{(0)}/\partial \zeta \pm f' \partial v^{(0)}/\partial \zeta \end{aligned}\right\} \quad \text{at} \quad y = \pm f(x). \tag{12}$$

A singular corner region permits a discontinuity between the variables evaluated on adjacent walls.

Matching the solutions in the core the side layers will provide additional boundary conditions. The formal matching procedure is very simple: it reduces to equating the limit of a core variable as $z \to \pm 1$ to that of the corresponding side-layer variable as $\zeta \to \mp \infty$. In other words, the ways in which these limits are approached do not enter the matching as far as we take it.

The first obvious results are

$$w^{(0)} = j_x^{(0)} = j_y^{(0)} = 0 \quad \text{and} \quad j_z^{(i)} = -dh^{(i)}/dx,$$

so that, in particular, the core solution satisfies $W^{(0)} = 0$ at $z = \pm 1$. Thus

$$h^{(0)} = C_1 x - C_2 \int_0^x f^{-1} dx, \quad \psi^{(0)} = 0, \tag{13}$$

where inessential additive constants have been omitted. The integration constants C_1 and C_2 are related to the pressure drop Nh_0 along the duct and the potentials $\mp \phi_0$ of the side walls $z = \pm 1$:

$$h_0 = -C_1 l + C_2 \int_0^l f^{-1} dx, \quad \phi_0 = C_1.$$

They are determined by the flux condition (2) and the external electrical circuit. If the side walls are connected by a resistance $\mathscr{R}/\sigma d$, the constants become

$$C_1 = C_2 \mathscr{R} l \left(1 + \mathscr{R} \int_0^l f dx\right)^{-1} \quad \text{and} \quad C_2 = f(0). \tag{13'}$$

It follows that the $O(1)$ core solution is simply

$$\left.\begin{aligned} &U^{(0)} = C_2 f^{-1}, \quad V^{(0)} = C_2 y f' f^{-2}, \quad W^{(0)} = 0, \\ &J_x^{(0)} = J_y^{(0)} = 0, \quad J_z^{(0)} = C_2 f^{-1} - C_1, \quad \Phi^{(0)} = -C_1 z, \end{aligned}\right\} \tag{14}$$

as found by Hunt & Leibovich (1967) who, because they looked for a solution in which $W^{(0)} = \partial/\partial z = 0$ and the electric field is transverse, did not need to apply the Hartmann condition (9*b*). Note that the $O(M^{-\frac{1}{2}})$ core variables in (10) are, as yet, not completely determined.

The equations

$$\partial j_x^{(\frac{1}{2})}/\partial y = \partial^3 v^{(0)}/\partial \zeta^3, \quad \partial j_y^{(\frac{1}{2})}/\partial y = -\partial^3 u^{(0)}/\partial \zeta^3, \tag{15a}$$

$$\partial j_x^{(\frac{1}{2})}/\partial \zeta = \partial v^{(0)}/\partial y - C_2 f' f^{-2}, \quad \partial j_y^{(\frac{1}{2})}/\partial \zeta = -\partial u^{(0)}/\partial y \tag{15b}$$

of the system (11) determine the non-trivial structure of the side-wall layers. The associated boundary conditions are

$$u^{(0)} = v^{(0)} = j_x^{(\frac{1}{2})} = j_y^{(\frac{1}{2})} = 0 \quad \text{at} \quad \zeta = 0; \tag{15c}$$

$$f' u^{(0)} \mp v^{(0)} = 0, \quad f' j_x^{(\frac{1}{2})} \mp j_y^{(\frac{1}{2})} = \partial u^{(0)}/\partial \zeta \pm f' \partial v^{(0)}/\partial \zeta \quad \text{at} \quad y = \pm f(x); \tag{15d}$$

and

$$u^{(0)} = C_2 f^{-1}, \quad v^{(0)} = C_2 y f' f^{-2}, \quad j_x^{(\frac{1}{2})} = j_y^{(\frac{1}{2})} = 0 \quad \text{at} \quad \zeta = \mp\infty. \tag{15e}$$

Once $u^{(0)}$ and $v^{(0)}$ have been found (which is the subject of the next section), the remaining equation of the set (11) yields

$$w^{(\frac{1}{2})} = -\int_0^{\zeta} (\partial u^{(0)}/\partial x + \partial v^{(0)}/\partial y)\, d\zeta. \tag{16}$$

It turns out that

$$w^{(\frac{1}{2})} = 0 \quad \text{at} \quad \zeta = \mp\infty, \tag{17}$$

so that $W^{(\frac{1}{2})} = 0$ at $z = \pm 1$ and this determines the remaining functions in the core solution:

$$h^{(\frac{1}{2})} = C_1' x - C_2' \int_0^x f^{-1} dx, \quad \psi^{(\frac{1}{2})} = 0.$$

Inessential additive constants have been omitted. The integration constants C_1' and C_2' are in fact zero, since otherwise the external resistance is changed and/or the flux condition (2) is violated, to order $M^{-\frac{1}{2}}$, as the following shows.

For $f' \neq 0$ we shall find, in contrast to the case $f' = 0$ studied by Hunt & Stewartson (1965), no flux deficiency in the side-wall layers, i.e. the displacement thickness of each layer is zero. Consequently, the correct value is obtained for the integral in condition (2), to order $M^{-\frac{1}{2}}$, if u is replaced by its core approximation $U^{(0)} + M^{-\frac{1}{2}} U^{(\frac{1}{2})} = -(C_2 + M^{-\frac{1}{2}} C_2')/f$; hence

$$C_2' = 0 \quad \text{for} \quad f' \neq 0.$$

The calculation of the current entering or leaving the side walls and of the potential difference between them is the same for $h^{(\frac{1}{2})}$ as it was for $h^{(0)}$. As a result, the first of the relations (13′) must also hold for C_1' and C_2', so that

$$C_1' = 0 \quad \text{for} \quad f' \neq 0.$$

In short, there is no $O(M^{-\frac{1}{2}})$ flow in the core and the Hunt–Leibovich solution (14) is correct to $O(M^{-1})$, as they supposed.

3. The governing integral equation of the side-wall layers

There remain the boundary-value problems (15), and by symmetry we need only consider the layer at $z = -1$, for which ζ is positive. It is convenient to write

$$\left.\begin{aligned} u^{(0)} &= C_2 f^{-1}(1 - f^{\frac{1}{2}}\partial\theta/\partial\zeta), & j_y^{(\frac{1}{2})} &= C_2 f^{-\frac{1}{2}}\partial\theta/\partial y, \\ v^{(0)} &= C_2 f' f^{-1}(yf^{-1} - f^{\frac{1}{2}}\partial\omega/\partial\zeta), & j_x^{(\frac{1}{2})} &= -C_2 f' f^{-\frac{1}{2}}\partial\omega/\partial y, \end{aligned}\right\} \tag{18}$$

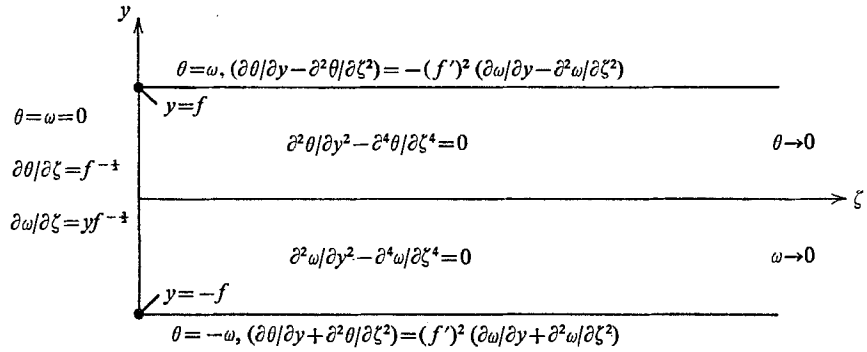

FIGURE 3. Boundary-value problem for side-wall layer.

so as to satisfy (15*b*) and to have variations θ, ω from core values. The resulting boundary-value problem for θ and ω is shown in figure 3. The left-end conditions suggest that θ is even and ω odd in y, and this assumption is compatible with the differential equations and remaining boundary conditions.

With the introduction of sine transforms

$$(\ \ ) = 2\pi^{-1}\int_0^\infty \sin(\xi\zeta)\,\overline{(\ \ )}\,d\xi,$$

the governing equations become

$$\partial^2\overline{\theta}/\partial y^2 - \xi^4\overline{\theta} = \xi F(y;x), \quad \partial^2\overline{\omega}/\partial y^2 - \xi^4\overline{\omega} = \xi G(y;x), \tag{19a}$$

where F and G are the unknown values of $\partial^2\theta/\partial\zeta^2$ and $\partial^2\omega/\partial\zeta^2$ on $\zeta = 0$, these functions being even and odd in y respectively. Similarly, the conditions on the top and bottom walls become

$$\overline{\theta} \mp \overline{\omega} = (\xi^2\overline{\theta} \pm \partial\overline{\theta}/\partial y) \pm (f')^2(\xi^2\overline{\omega} \pm \partial\overline{\omega}/\partial y) = 0 \quad \text{at} \quad y = \pm f(x). \tag{19b}$$

The solution $\overline{\theta}, \overline{\omega}$ of the boundary-value problem (19*a*, *b*) will contain the functions F and G. By making it satisfy the left-end conditions

$$\partial\theta/\partial\zeta = 2\pi^{-1}\int_0^\infty \overline{\theta}\xi\,d\xi = f^{-\frac{1}{2}}, \quad \partial\omega/\partial\zeta = 2\pi^{-1}\int_0^\infty \overline{\omega}\xi\,d\xi = yf^{-\frac{3}{2}}, \tag{19c}$$

which have so far not been applied, integral equations will result for F and G. For this purpose it is convenient to introduce the new variables

$$Y = yf^{-1}, \quad \Xi = \xi f^{\frac{1}{2}}, \quad \text{and the parameter} \quad \beta = (1 - f'^2)/(1 + f'^2). \tag{20}$$

Then

$$\bar{\theta} = \tfrac{1}{2}(\bar{R}(+Y)+\bar{R}(-Y)), \quad \bar{\omega} = \tfrac{1}{2}(\bar{R}(+Y)-\bar{R}(-Y)), \tag{21}$$

where

$$\left.\begin{aligned} \bar{R} &= \pi^{\frac{1}{2}} f^{\frac{1}{2}} \Xi^{-1} \int_{-1}^{+1} r(Y^*;\beta)\,(\bar{K}(Y, Y^*, \Xi;\beta) - \exp(-\Xi^2|Y-Y^*|))\,dY^*, \\ \bar{K} &= \exp(-\Xi^2(2+Y+Y^*))\,(1-\beta\exp(2\Xi^2 Y))/(1-\beta\exp(-2\Xi^2)), \end{aligned}\right\} \tag{21'}$$

and

$$r = \tfrac{1}{2}\pi^{-\frac{1}{2}} f(F+G).$$

This solution will satisfy the conditions (19c) if r satisfies the integral equation

$$1+Y = \int_{-1}^{+1} r(Y^*;\beta)\left(2\pi^{-\frac{1}{2}}\int_0^\infty \bar{K}(Y, Y^*, \Xi;\beta)\,d\Xi - |Y-Y^*|^{-\frac{1}{2}}\right) dY^*. \tag{22}$$

The entire problem then is to solve this equation for r, which gives F and G from its even and odd parts in y. Once this has been done, $\bar{\theta}, \bar{\omega}$ follow the formulas (21), so that on inversion

$$\theta = \tfrac{1}{2}(R(+Y)+R(-Y)), \quad \omega = \tfrac{1}{2}(R(+Y)-R(-Y)), \tag{23}$$

where

$$R = \pi^{\frac{1}{2}} \int_{-1}^{+1} r(Y^*;\beta)\,(K(Y, Y^*, Z;\beta) - \operatorname{erf}(\tfrac{1}{2}Z|Y-Y^*|^{-\frac{1}{2}}))\,dY^*, \tag{23'}$$

$$K = 2\pi^{-1}\int_0^\infty \sin(Z\Xi)\,\bar{K}(Y, Y^*, \Xi;\beta)\,\Xi^{-1}\,d\Xi, \quad \text{and} \quad Z = \zeta f^{-\frac{1}{2}}. \tag{23''}$$

The velocities and currents are then given by

$$u^{(0)} = C_2 f^{-1}(1-\partial\theta/\partial Z), \quad v^{(0)} = C_2 f' f^{-1}(Y-\partial\omega/\partial Z), \tag{24a,b}$$

$$j_x^{(\frac{1}{2})} = -C_2 f' f^{-\frac{3}{2}}\partial\omega/\partial Y, \quad j_y^{(\frac{1}{2})} = C_2 f^{-\frac{3}{2}}\partial\theta/\partial Y, \tag{24c,d}$$

$$w^{(\frac{1}{2})} = C_2 f' f^{-\frac{3}{2}} W_1 + C_2\beta' f^{-\frac{1}{2}} W_2, \tag{24e}$$

where

$$W_1 = \partial\omega/\partial Y - \tfrac{1}{2}\theta - \tfrac{1}{2}Z\,\partial\theta/\partial Z - Y\partial\theta/\partial Y, \quad W_2 = \partial\theta/\partial\beta.$$

Clearly, this gives the value (17) anticipated in the last section.

4. Boundary-layer profiles

Except for the cases $\beta = 0$ and 1, which are discussed in the next section, the integral equation (22) must apparently be solved numerically. But first troublesome singularities are eliminated by several simple changes. (i) The term $|Y-Y^*|^{-\frac{1}{2}}$ is removed by integration with respect to Y between -1 and a new variable Y. Although the integrated kernel is then finite everywhere, its slope is infinite along the diagonal $Y = Y^*$. The Gauss-quadrature approximation is therefore improved if the function

$$\int_{-1}^{+1} r(Y;\beta)\,(-2\operatorname{sgn}(Y-Y^*)|Y-Y^*|^{\frac{1}{2}})\,dY^* = \tfrac{4}{3}r(Y;\beta)\,((1-Y)^{\frac{3}{2}} - (1+Y)^{\frac{3}{2}})$$

is subtracted from the integral. (ii) In evaluating

$$\int_{-1}^{Y}\int_{0}^{\infty} \bar{K}(Y', Y^*, \Xi; \beta)\, d\Xi\, dY',$$

part of $\bar{K}$ is removed and integrated exactly over the semi-infinite range of Ξ; so that the remaining integrand behaves like $\exp(-2\Xi^2)$ for large Ξ and any Y and Y^*. Gauss–Hermite quadrature can then be used for the portion of the range beyond some Ξ_0. Because of the factor Ξ^{-2}, integration by parts is used in the range $(0, \Xi_0)$ before Gauss quadrature is applied. (iii) Since r behaves like $(1-Y^*)^{-\frac{1}{4}}$ near $Y^* = +1$, the integral is rescaled with

$$Y^* = 1 - 2^{-\frac{1}{3}}(1-\tilde{Y})^{\frac{4}{3}} \quad \text{and} \quad r = \tfrac{3}{4} \times 2^{\frac{1}{4}}(1-Y^*)^{-\frac{1}{4}}\tilde{r}.$$

The resulting kernel is approximated by a matrix of its values at specific $(Y, \tilde{Y})$ points. The ordinates $\tilde{Y}$ have 24 Gauss-quadrature values, while the abscissas Y are chosen to give a symmetric array in the Y, Y^* plane. In this way the diagonal $Y = Y^*$ is covered. The set of linear equations (containing the Gauss weight factors) which approximates the integral equation (22) is then solved for the values of $\tilde{r}$ at the discrete $\tilde{Y}$ values. The function $\partial r/\partial\beta$, which is needed for $w^{(\frac{1}{2})}$, is determined by the same scheme with the function $1+Y$ replaced by an integral of r.

These two functions are then integrated numerically to give the velocity and current profiles in the boundary layers. With proper scaling (see equations (24*a–d*)) the components $u^{(0)}$, $v^{(0)}$, $j_x^{(\frac{1}{2})}$, and $j_y^{(\frac{1}{2})}$ depend on x only through the divergence parameter $\beta(x)$. On the other hand (see equation (24*e*)), $w^{(\frac{1}{2})}$ must be divided into two functions which can be scaled separately into profiles determined by $\beta(x)$.

Several typical profiles are given in figure 4. Figure 4(*a*) shows the variation with β of the velocity $u^{(0)}$ on the line of symmetry $y = 0$. The crossed points $\times$ are the results of Hunt & Stewartson (1965) for the constant-area duct, $\beta \equiv 1$. The solution for $\beta = -1$ can be used for a duct with $|f'| \gg 1$, as long as the approximations made in deriving the integral equation (22) remain valid. The slope enters only in the conditions (15*d*), and these are still a consequence of the Hartmann conditions whenever $|f'| \ll M$. The other plots in figure 4 give profiles for the velocities and currents at the levels $Y = 0{\cdot}25, 0{\cdot}75$ of a cross-section where the wall slope is two ($\beta = -0{\cdot}60$).

In particular, we note the overshoot which occurs in each of the profiles of figure 4(*a*) with the exception of $\beta = 1$. This is connected with the absence of a flux deficiency in the side layer; a result which can be proved without reference to the side-layer structure. Any solution of equations (1*b*, *d*) with $w = 0$ and constant potential on $z = \pm 1$ will satisfy

$$\frac{\partial}{\partial y}\int_{-1}^{1} u\,dz = \frac{\partial}{\partial y}\int_{-1}^{1} j_z dz \quad \text{and} \quad \frac{\partial}{\partial y}\int_{-1}^{1} v\,dz = -\frac{\partial}{\partial x}\int_{-1}^{1} j_z dz. \tag{25}$$

In particular we may set u, v, j_z equal to $u^{(0)}$, $v^{(0)}$, $j_z^{(0)}$ or $U^{(0)}$, $V^{(0)}$, $J_z^{(0)}$ and hence their difference $\hat{u}^{(0)}$, $\hat{v}^{(0)}$, $\hat{j}_z^{(0)}$. Since $\hat{j}_z^{(0)} = 0$ we therefore have

$$\int_{-1}^{1} \hat{u}^{(0)} dz = \mathscr{F}(x) \quad \text{and} \quad \int_{-1}^{1} \hat{v}^{(0)} dz = \mathscr{H}(x).$$

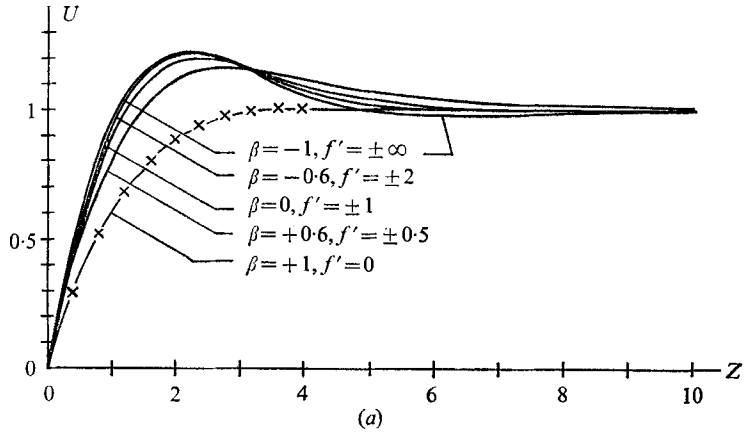

(a)

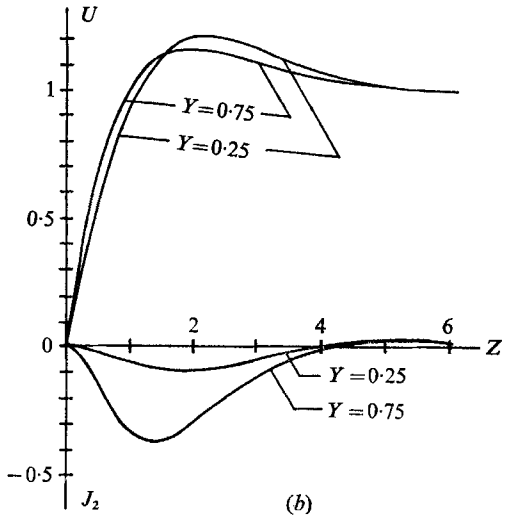

(b)

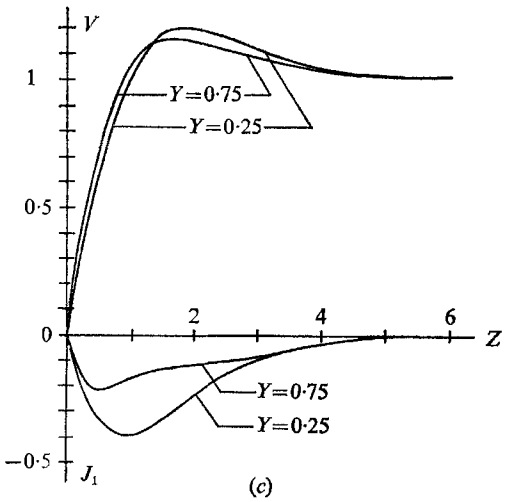

(c)

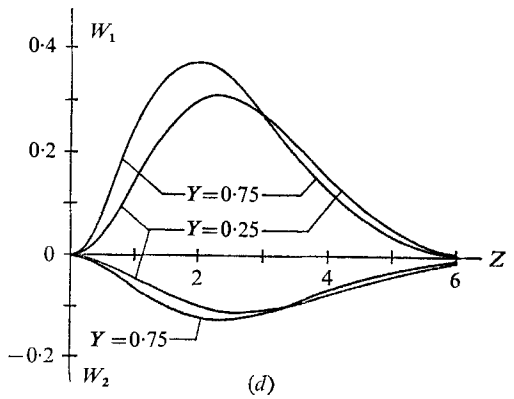

(d)

FIGURE 4. Boundary-layer profiles for parallel side walls, showing overshoots for $f' \neq 0$.
(a) $u^{(0)} = C_2 f^{-1} U$ at $y = 0$ for various values of f'. Crosses show Hunt & Stewartson's values for a constant-area duct.

$$\left.\begin{array}{ll} (b) & u^{(0)} = C_2 f^{-1} U \quad \text{and} \quad j_y^{(\frac{1}{2})} = C_2 f^{-\frac{3}{2}} J_2 \\ (c) & v^{(0)} = C_2 f' Y f^{-1} V \quad \text{and} \quad j_x^{(\frac{1}{2})} = C_2 f' f^{-\frac{3}{2}} J_1 \\ (d) & w^{(0)} = C_2 f' f^{-\frac{3}{2}} W_1 + C_2 \beta' f^{-\frac{1}{2}} W_2 \end{array}\right\} \quad \text{for} \quad f' = \pm 2.$$

Now, whatever the structure of the side layers, the normal component of the $O(1)$ velocity must vanish at the top and bottom:

$$f'\hat{u}^{(0)} \mp \hat{v}^{(0)} = 0 \quad \text{at} \quad y = \pm f(x).$$

Integrating this between the side walls $z = \pm 1$ then gives

$$f'\mathscr{F} \mp \mathscr{H} = 0, \quad \text{i.e.} \quad \mathscr{F}(x) \equiv \mathscr{H}(x) \equiv 0 \quad \text{when} \quad f' \neq 0.$$

Thus the $O(M^{-\frac{1}{2}})$ flux deficiency is identically zero at each level $y = \text{const.}$ and the velocity profiles derived from the solution of the integral equation (22) will have this property for all $\beta \neq 1$. When $\beta = 1$ there is a flux deficiency, as was noted by Hunt & Stewartson (1965), and the paradox will be explained in the next section.

5. Special divergences: $\beta = 0, 1$

Exact analysis is possible for two values of the divergence parameter $\beta(x)$. For $\beta = 0$ ($f' = \pm 1$), the integral equation (22) reduces to

$$1 + Y = \int_{-1}^{+1} r(Y^*; 0)\,[(2 + Y + Y^*)^{-\frac{1}{2}} - |Y - Y^*|^{-\frac{1}{2}}]\,dY^*. \tag{26}$$

In terms of the function

$$q(\tau) = \begin{cases} r((1-4\tau); 0) & \text{for} \quad 0 \leqslant \tau \leqslant \frac{1}{2}, \\ -r((4\tau-3); 0) & \text{for} \quad \frac{1}{2} \leqslant \tau \leqslant 1, \end{cases} \tag{27}$$

this equation becomes

$$2\tau - 1 = \int_0^{+1} q(\tau^*)|\tau - \tau^*|^{-\frac{1}{2}}\,d\tau^*, \quad \text{for} \quad 0 \leqslant \tau \leqslant 1,$$

which has been solved by Carleman (1922) and others. The solution gives

$$r(Y; 0) = -2^{\frac{1}{2}}\pi^{-1}(1-Y)^{-\frac{1}{4}}(3+Y)^{-\frac{1}{4}}(1+Y).$$

The corresponding functions θ, ω are defined by substituting this solution into equation (23′), with K simplified for $\beta = 0$. This integral could not be found, so explicit expressions for the velocity and current profiles cannot be written.

The flow for small β can be obtained by using this solution as the first term of a power series in β. If

$$r(Y; \beta) = \sum_{i=0}^{\infty} \beta^i r_i(Y),$$

each term $r_i(Y)$ is governed by the same integral equation (26) with the function $1 + Y$ replaced by an integral of the previous terms. The solution for any r_i can finally be written as a single weighted integral of the known function $r(Y; 0)$. For instance,

$$r_1(Y) = 2^{-\frac{1}{2}}\pi^{-1}(1-Y)^{-\frac{1}{4}}(3+Y)^{-\frac{1}{4}} \int_{-1}^{+1} r(Y^*; 0)\,(1+Y^*)^{\frac{1}{4}}(5+Y^*)^{\frac{1}{4}} \times ((4 + Y^* + Y)^{-1} - (2 + Y^* - Y)^{-1})\,dY^*.$$

The first two terms provide a check on the numerical solution for r and $\partial r/\partial\beta$ when $\beta = 0$.

The solution for $\beta = 1$ describes the fully developed flow in a constant-area duct and should agree with the previous results for this special case. Then $f(x) = f(0)$ so that $v^{(0)}$ and $j_x^{(\frac{1}{2})}$ are zero, and ω is an irrelevant odd function of y. The flow is therefore governed by the even part of the integral equation (22),

$$2\pi^{\frac{1}{2}} = \int_{-f}^{+f} \partial u^{(0)}/\partial\zeta(0, y^*, x)|y - y^*|^{-\frac{1}{2}} dy^*,$$

which has the solution

$$\partial u^{(0)}/\partial\zeta(0, y, x) = (2/\pi)^{\frac{1}{2}}(f^2 - y^2)^{-\frac{1}{4}}.$$

This is the result given by Chiang & Lundgren (1967) in the appendix of their paper. Both they and Hunt & Stewartson (1965) use an alternative approach to the problem, which, in terms of the present analysis, is equivalent to using cosine transforms. Then left-end conditions $\theta = \omega = 0$ give integral equations on the unknown values of $\partial^3\theta/\partial\zeta^3$ and $\partial^3\omega/\partial\zeta^3$ on $\zeta = 0$. Of course the two approaches give completely equivalent solutions to the governing equations.

However, they find a flux deficiency in the boundary layer which is absent from our solution for every value of $\beta \neq 1$. The apparent contradiction is best demonstrated by splitting the velocity down the duct into three parts and considering the behaviour of each as $\beta \to 1$. From equation (23) we have

$$u^{(0)} = C_2 f^{-1}(u_1 + u_2 + u_3),$$

where

$$u_1 = 1 + \tfrac{1}{2}\int_{-1}^{+1} (r(Y^*;\beta) + r(-Y^*;\beta))\,|Y - Y^*|^{-\frac{1}{2}} \exp(-\tfrac{1}{4}Z^2|Y - Y^*|^{-1})\,dY^*,$$

$$u_2 = -(\pi/2)^{\frac{1}{2}}(1-\beta)^{\frac{1}{2}} \exp(-Z(1-\beta)^{\frac{1}{2}}2^{-\frac{1}{2}}) \int_{-1}^{+1} r(Y^*;\beta)\,dY^*,$$

$$u_3 = -2\pi^{-\frac{1}{2}}(1-\beta)\int_{-1}^{+1} r(Y^*;\beta)\,U_3(Z, Y, Y^*;\beta)\,dY^*,$$

and

$$U_3 = \int_0^\infty \cos(Z\Xi)\,(\cosh(\Xi^2 Y) \exp(-\Xi^2 Y^*)\,(\exp(2\Xi^2) - \beta^{-1}) - (1 - \beta + 2\Xi^2)^{-1})\,d\Xi.$$

The sum $u_2 + u_3$ gives the contribution due to K. The extra term $(1 - \beta + 2\Xi^2)^{-1}$ in U_3 ensures that the integral is finite for all β; otherwise it behaves like $(1-\beta)^{-\frac{1}{2}}$ as $\beta \to 1$. In addition it is chosen to give

$$\int_0^\infty u_3\,dZ = 0$$

for each Y and every β, and to yield a simple compensating function u_2. We find

$$\int_0^\infty u_2\,dZ = -\pi^{\frac{1}{2}}\int_{-1}^{+1} r(Y^*;\beta)\,dY^* \quad \text{and} \quad \int_0^\infty (u_1 - 1)\,dZ = \pi^{\frac{1}{2}}\int_{-1}^{+1} r(Y^*;\beta)\,dY^*$$

for each Y and every β.

In the limit $\beta \to 1$ the velocity profile is given by u_1 alone, the contributions from u_2 and u_3 being zero. Nevertheless, however close β is to 1, u_2 provides a non-zero total flux which exactly cancels the flux deficiency due to u_1.

The function u_2 also shows the nature of the transition from our result to that of Hunt & Stewartson. As $\beta \to 1$ it becomes uniformly small over the whole range of Z, but it ceases to be exponentially small in the core for $(1-\beta) = O(M^{-1})$, when it induces an $O(M^{-\frac{1}{2}})$ perturbation there. We may visualize the overshoot for $f' \gg M^{-\frac{1}{2}}$ as moving steadily towards the edge of the side layer until for $f' = O(M^{-\frac{1}{2}})$ it penetrates the core.

It is now clear that the fully developed solution of Hunt & Stewartson is not typical of flow in a rectangular duct. When the duct is converging or diverging the side-wall layers have no flux deficits and there is no $O(M^{-\frac{1}{2}})$ disturbance of the core flow. Only near a throat where f' becomes comparable to $M^{-\frac{1}{2}}$, is fluid forced out of the side-wall layers into the centre of the duct. It would be interesting to determine the flow in the transition region where f' changes from being comparable to $M^{-\frac{1}{2}}$ to being large compared to it.

6. Diverging side walls

The success of the preceding analysis is due to the fact that the core solution, given by $i = 0$ in (10) automatically satisfies the electromagnetic part of the side boundary conditions (3*b*). The side layers do not have to accommodate a jump in the tangential current. When the side walls diverge, however, $J_z^{(0)}$ has a component parallel to a side wall, and this must be reduced to zero across the layer. The resulting $O(M^{\frac{1}{2}})$ gradients in current imply, according to equation (4*b*), velocities of the same order. The total flux through the duct is now distributed between the core flow and the $O(M^{\frac{1}{2}})$ flows in the side layers.

To allow for such velocities in the side layers the expansion (6) is replaced by

$$u = u^{(-\frac{1}{2})}M^{\frac{1}{2}} + u^{(0)} + O(M^{-\frac{1}{2}}).$$

In the core, the $O(M^{\frac{1}{2}})$ variables are all zero and the $O(1)$ are given by (10) with $i = 0$; the integration functions $h^{(0)}(x)$ and $\psi^{(0)}(x)$ have to be determined by matching with the layers on the side walls, now taken to be

$$z = \pm g(x) \quad \text{with} \quad g(0) = 1.$$

Note that the characteristic length d is henceforth the half-width at $x = 0$ and the condition (2) still holds.

By symmetry we need only consider the layer at $z = -g(x)$. It is convenient to introduce, at the x station considered, the local Cartesian co-ordinates $\tilde{x}, y, \tilde{z}$ shown in figure 5. The $\tilde{x}$ direction is parallel to the wall while the $\tilde{z}$ is perpendicular to it, so that now $\zeta = M^{\frac{1}{2}}\tilde{z}$. The components of velocity and current are referred to this local system; for example, $\tilde{u}^{(-\frac{1}{2})}$ is the $O(M^{\frac{1}{2}})$ horizontal velocity parallel to the wall. When tildes are applied appropriately and the superscripts $\frac{1}{2}$, 0 changed to 0, $-\frac{1}{2}$, we find that the governing equations (15*a*, *b*) and the side-wall conditions (15*c*) still hold, while the Hartmann conditions (15*d*) become

$$\left.\begin{aligned} &\alpha f'\tilde{u}^{(-\frac{1}{2})} \mp v^{(-\frac{1}{2})} + \alpha f' g' \tilde{w}^{(-\frac{1}{2})} = \alpha f' j_{\tilde{x}}^{(-\frac{1}{2})} \mp j_y^{(-\frac{1}{2})} + \alpha f' g' j_{\tilde{z}}^{(-\frac{1}{2})} = 0 \\ &\alpha f' j_{\tilde{x}}^{(0)} \mp j_y^{(0)} + \alpha f' g' j_{\tilde{z}}^{(0)} = \partial \tilde{u}^{(-\frac{1}{2})}/\partial\zeta \pm a f' \partial v^{(-\frac{1}{2})}/\partial\zeta \end{aligned}\right\} \quad \text{at} \quad y = \pm f(x), \quad (28)$$

where $$\alpha = (1+g'^2)^{-\frac{1}{2}}.$$

But it is the boundary conditions as $\zeta \to \infty$, which come from matching with the core solution, that change the layer problem.

The first obvious results are

$$\tilde{w}^{(-\frac{1}{2})} = \mathbf{j}^{(-\frac{1}{2})} = 0 \quad \text{and} \quad j_{\tilde{z}}^{(0)} = -\alpha\, dh^{(0)}/dx. \tag{29}$$

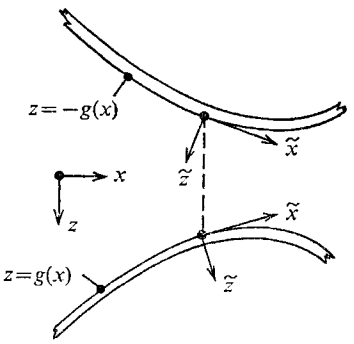

FIGURE 5. y section showing local co-ordinates $\tilde{x}$, $\tilde{z}$ for each side wall.

We must then consider the equations

$$\partial j_{\tilde{x}}^{(0)}/\partial y = \partial^3 v^{(-\frac{1}{2})}/\partial \zeta^3, \quad \partial j_{\tilde{x}}^{(0)}/\partial \zeta = \partial v^{(-\frac{1}{2})}/\partial y,$$
$$\partial j_y^{(0)}/\partial y = -\partial^3 \tilde{u}^{(-\frac{1}{2})}/\partial \zeta^3, \quad \partial j_y^{(0)}/\partial \zeta = -\partial \tilde{u}^{(-\frac{1}{2})}/\partial y$$

under the boundary conditions (28), with the results (29) inserted, and

$$\tilde{u}^{(-\frac{1}{2})} = v^{(-\frac{1}{2})} = j_{\tilde{x}}^{(0)} = j_y^{(0)} = 0 \quad \text{at} \quad \zeta = 0,$$
$$\tilde{u}^{(-\frac{1}{2})} = v^{(-\frac{1}{2})} = 0, \quad j_{\tilde{x}}^{(0)} = \alpha g' dh^{(0)}/dx, \quad j_y^{(0)} = 0 \quad \text{at} \quad \zeta = \infty.$$

Once $\tilde{u}^{(-\frac{1}{2})}$ and $v^{(-\frac{1}{2})}$ have been determined, $\tilde{w}^{(0)}$ can be found by the ζ integration (16).

It turns out that

$$\tilde{w}^{(0)} = -\alpha \left[\frac{d}{dx}\left(\frac{g'f}{f'} \frac{dh^{(0)}}{dx} \right) + g' \frac{dh^{(0)}}{dx} \right] \quad \text{at} \quad \zeta = \infty, \tag{30}$$

and the core velocity normal to the wall,

$$\tilde{W}^{(0)} = \alpha \left[\frac{g'f}{f'} \frac{d^2h^{(0)}}{dx^2} + \frac{d\psi^{(0)}}{dx} + g \frac{d}{dx} \left\{ \frac{1}{f'} \frac{d}{dx} \left(f \frac{dh^{(0)}}{dx} \right) \right\} \right],$$

must equal it. A similar result, with g changed to $-g$, arises from the other side layer, so that the integration functions in the core solution are now determined:

$$h^{(0)} = C_1 \int_0^x g^{-1}\, dx - C_2 \int_0^x f^{-1} g^{-1}\, dx, \quad \psi^{(0)} = 0. \tag{31}$$

Inessential additive constants have been omitted. As before, the integration constants C_1 and C_2 are related to the pressure drop Nh_0 along the duct and the potentials $\mp \phi_0$ of the side walls $z = \pm g$:

$$h_0 = -C_1 \int_0^l g^{-1}\, dx + C_2 \int_0^l f^{-1} g^{-1}\, dx, \quad \phi_0 = C_1.$$

They are determined by the flux condition (2) and the external electric circuit. When account is taken of the change in potential across the side layers and of the flux down them, we find

$$C_1 = C_2\mathscr{R}\left(\int_0^l g^{-1}dx\right)\left(1+\mathscr{R}\int_0^l fg^{-1}dx\right)^{-1}, \quad C_2 = f(0), \tag{31'}$$

for side walls connected by a resistance $\mathscr{R}/\sigma d$. In particular we note that the $O(1)$ core flow, given by equations (10) with $i = 0$, reduces to the previous one, given by equations (14), when $g \equiv 1$.

The $O(1)$ core solution (10) is no longer of the Hunt–Leibovich type; in particular there is now a transverse velocity. Moreover, for $g' \neq 0$, $d^2h^{(0)}/dx^2$ no longer has a factor f', so that the solution becomes singular as $f' \to 0$ and does not reduce to that for $f' \equiv 0$ [cf. the remark after equation (10')]. This is not surprising, since the latter has a quite different form, as we shall see in the next section.

There remains the boundary-value problem mentioned above, for which it is convenient to write

$$\tilde{w}^{(-\frac{1}{2})} = -\frac{g'f}{f'}\frac{dh^{(0)}}{dx}\frac{\partial\theta}{\partial\zeta}, \quad v^{(-\frac{1}{2})} = -\alpha g' f\frac{dh^{(0)}}{dx}\frac{\partial\omega}{\partial\zeta},$$

$$j_x^{(0)} = \alpha g'\frac{dh^{(0)}}{dx}\left(1-f\frac{\partial\omega}{\partial y}\right), \quad j_y^{(0)} = \frac{g'f}{f'}\frac{dh^{(0)}}{dx}\frac{\partial\theta}{\partial y};$$

correspondingly

$$\tilde{w}^{(0)} = \alpha\left[\frac{\partial}{\partial x}\left\{\frac{g'f}{f'}\frac{dh^{(0)}}{dx}(\theta-1)\right\}+g'\frac{dh^{(0)}}{dx}\left(f\frac{\partial\omega}{\partial y}-1\right)\right].$$

Once more figure 3 shows the problem for θ and ω, except that f' must be replaced by $\alpha f'$ and the conditions at $\zeta = 0$ by

$$\theta = 1, \quad \omega = y/f, \quad \partial\theta/\partial\zeta = \partial\omega/\partial\zeta = 0.$$

The analysis parallels that of § 3, except that cosine transforms are used instead of sine to take account of the changed boundary conditions at $\zeta = 0$. In brief, we find

$$\theta = \tfrac{1}{2}(R(+Y)+R(-Y)), \quad \omega = \tfrac{1}{2}(R(+Y)-R(-Y)),$$

where

$$R = \pi^{\frac{1}{2}}\int_{-1}^{+1} r(Y^*;\beta)\,L(Y, Y^*, Z;\beta)\,dY^*$$

and

$$L = 2\pi^{-1}\int_0^\infty [\exp(-\Xi^2|Y-Y^*|)-\bar{K}(Y, Y^*, \Xi;\beta)]\cos(Z\Xi)\,d\Xi/\Xi^2,$$

$\bar{K}$ being defined by (21'). These should be compared with the formulas (23); in particular

$$\partial L/\partial Z = K - \operatorname{erf}(\tfrac{1}{2}Z|Y-Y^*|^{-\frac{1}{2}}).$$

Note that Y and Z are the scaled co-ordinates (20) and (23″) used previously, but that β is now generalized to

$$\beta = (1-\alpha^2f'^2)/(1+\alpha^2f'^2).$$

The function r which appears in these results is

$$r = \tfrac{1}{2}\pi^{-\frac{1}{2}} f^{\frac{3}{2}}(F+G),$$

where F and G are now the unknown values of $\partial^3\theta/\partial\zeta^3$ and $\partial^3\omega/\partial\zeta^3$ on $\zeta = 0$. It is to be determined from the integral equation

$$1+Y = \int_{-1}^{+1} r(Y^*;\beta)\left(2\pi^{-\frac{1}{2}}\int_0^\infty [\exp(-\Xi^2|Y-Y^*|) - \bar{K}(Y,Y^*,\Xi;\beta)]\frac{d\Xi}{\Xi^2}\right)dY^*,$$

which may be compared with the previous equation (22).

Once θ and ω have been found the velocities and currents are given by

$$\tilde{u}^{(-\frac{1}{2})} = -\frac{g'f^{\frac{1}{2}}}{f'}\frac{dh^{(0)}}{dx}\frac{\partial\theta}{\partial Z}, \quad v^{(-\frac{1}{2})} = -\alpha g' f^{\frac{1}{2}}\frac{dh^{(0)}}{dx}\frac{\partial\omega}{\partial Z},$$

$$j_x^{(0)} = \alpha g'\frac{dh^{(0)}}{dx}\left(1-\frac{\partial\omega}{\partial Y}\right), \quad j_y^{(0)} = \frac{g'}{f'}\frac{dh^{(0)}}{dx}\frac{\partial\theta}{\partial Y},$$

$$\tilde{w}^{(0)} = \alpha g'\frac{dh^{(0)}}{dx}W_1 + \alpha\beta'\frac{g'f}{f'}\frac{dh^{(0)}}{dx}W_2 + \alpha\frac{d}{dx}\left(\frac{g'f}{f'}\frac{dh^{(0)}}{dx}\right)W_3,$$

where

$$W_1 = \frac{\partial\omega}{\partial Y} - Y\frac{\partial\theta}{\partial Y} - \tfrac{1}{2}Z\frac{\partial\theta}{\partial Z} - 1, \quad W_2 = \frac{\partial\theta}{\partial\beta}, \quad W_3 = \theta - 1.$$

Clearly this gives the value (30) anticipated earlier.

The numerical determination of r and $\partial r/\partial\beta$ (which is needed for W_2) and the integration of these functions to obtain the velocity and current profiles follows closely the work described in § 4. As there, the profiles are described by functions depending on x only through β. This time, however, $\tilde{w}^{(0)}$ requires three such functions instead of two. Several typical profiles are given in figure 6. It is noteworthy that when β is negative there is a reversal in the $\tilde{u}^{(-\frac{1}{2})}$ profile near the centreline $y = 0$.

It is of particular interest to determine how much of the total flux through the duct is carried in the core. By integrating $\tilde{u}^{(-\frac{1}{2})}$ through the side layer or $U^{(0)}$ across the core, we find the fraction

$$Q_c(x) = 1 + \frac{fg'}{f'g}(1-\lambda), \quad \lambda(x;\mathscr{R}) = \frac{f\mathscr{R}\int_0^l g^{-1}dx}{1+\mathscr{R}\int_0^l fg^{-1}dx}. \tag{32}$$

A detailed discussion of this result will be given in § 8; but it is immediately clear from the case of short-circuited side walls ($\mathscr{R} = 0$) that there may actually be backflow in the core ($Q_c < 0$) or in the side layers ($Q_c > 1$).

One physical explanation is that sufficiently large values of g' create large potential jumps across the side layers. Since the potential between the side walls is zero, a strong field E_z is created which can drive the core flow backwards!

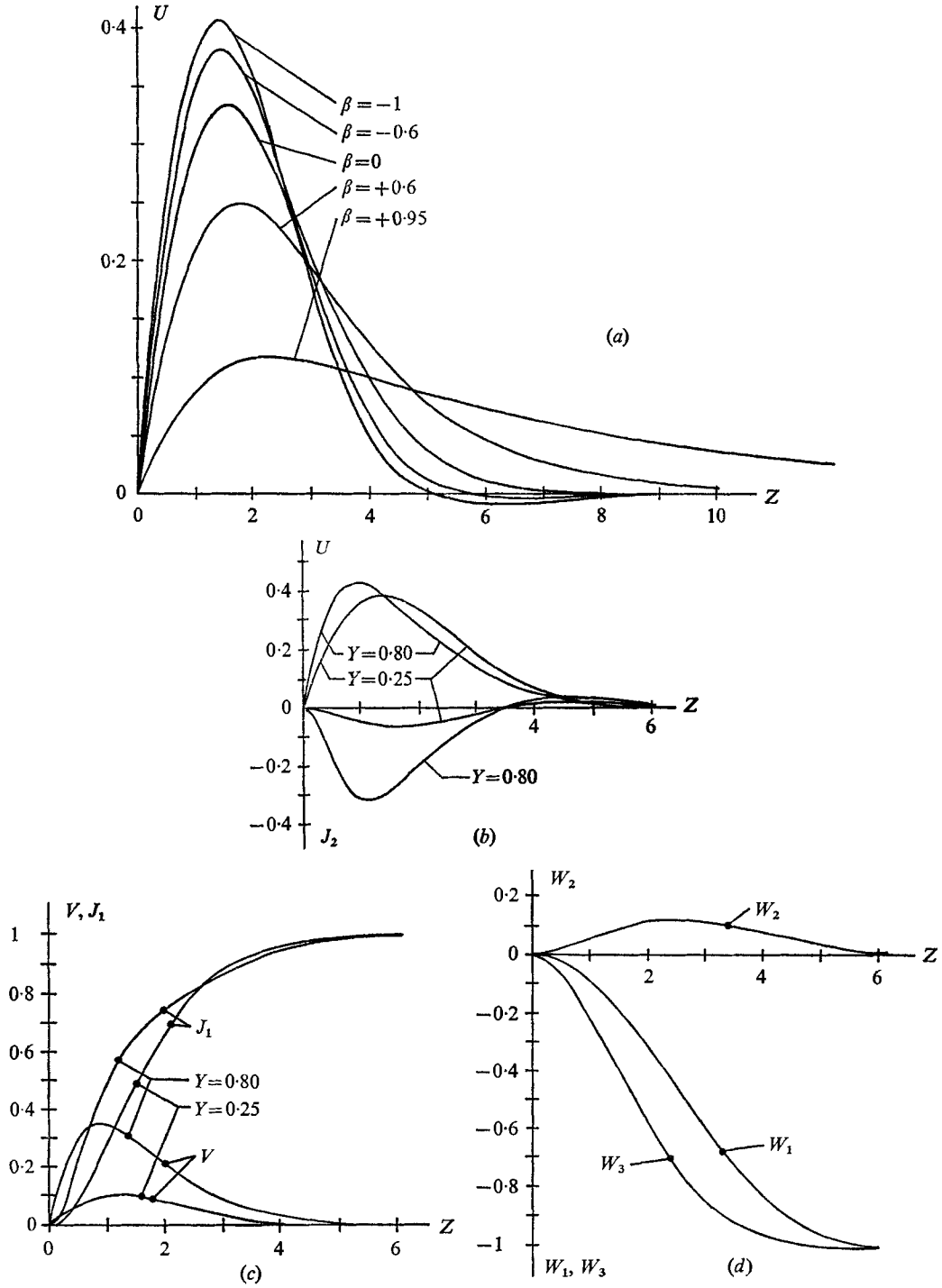

FIGURE 6. Boundary-layer profiles for diverging side walls.

(*a*) $\tilde{u}_{(-\frac{1}{2})} = f'^{-1}g'f^{\frac{1}{2}}(dh^{(0)}/dx)U$ at $y = 0$ for various values of β.

(*b*) $\tilde{u}^{(-\frac{1}{2})} = f'^{-1}g'f^{\frac{1}{2}}(dh^{(0)}/dx)U$ and $j_y^{(0)} = f'^{-1}g'(dh^{(0)}/dx)J_2$

(*c*) $v^{(-\frac{1}{2})} = \alpha g'f^{\frac{1}{2}}(dh^{(0)}/dx)V$ and $j_z^{(0)} = \alpha g'(dh^{(0)}/dx)J_1$

(*d*) $\tilde{w}^{(0)} = \alpha g'(dh^{(0)}/dx)W_1 + \alpha f'^{-1}g'\beta' f(dh^{(0)}/dx)W_2 + \alpha(f'^{-1}g'f(dh^{(0)}/dx))'W_3$

for $\beta = -0{\cdot}6$.

For the special case $\beta = 0$ the integral equation can be solved exactly. Thus

$$1 + Y = 2\int_{-1}^{+1} r(Y^*; 0)\,[(2 + Y + Y^*)^{\frac{1}{2}} - |Y - Y^*|^{\frac{1}{2}}]\,dY^*$$

and the same transformation (27) reduces this to a standard form from which we find

$$r(Y; 0) = 2^{-\frac{1}{2}}\pi^{-1}(1 - Y)^{-\frac{3}{4}}(3 + Y)^{-\frac{3}{4}}(1 + Y).$$

The result provides a useful check on the numerical solution for $\beta = 0$.

In general, the solution becomes singular for every non-zero g' as $f' \to 0$ (i.e. $\beta \to 1$), as can be seen from the flux formula (32). We shall return to this question in §7, where, in particular, implications for a duct with $f' \equiv 0$ will be discussed.

7. The exceptional case $f' \equiv 0$

To complete our discussion of flow in variable-area rectangular ducts with conducting side walls we consider the case in which the other walls are plane and parallel, i.e. $f' \equiv 0$. Part 1 pointed out that the two Hartmann conditions (9*b*) are then effectively a single condition, and that further examination of the Hartmann-layer condition (8*b*), to order M^{-1}, is needed to resolve the indeterminacy. Their argument applied whatever the shape and nature of the side walls and leads to the core solution

$$U^{(0)} = -\frac{\partial h^{(0)}}{\partial x} - \frac{\partial \phi^{(0)}}{\partial z}, \quad V^{(0)} = 0, \quad W^{(0)} = -\frac{\partial h^{(0)}}{\partial z} + \frac{\partial \phi^{(0)}}{\partial x},$$

$$J_x^{(0)} = \frac{\partial h^{(0)}}{\partial z}, \quad J_y^{(0)} = 0, \quad J_z^{(0)} = -\frac{\partial h^{(0)}}{\partial x}.$$

Here $h^{(0)}$, the pressure divided by N, and $\phi^{(0)}$, the electric potential, are harmonic functions of x, z and expansions of the type (6) are involved.

Such a core solution will have zero tangential current and zero normal velocity at the side walls in our problem if

$$g'\frac{\partial h^{(0)}}{\partial x} \mp \frac{\partial h^{(0)}}{\partial z} = 0 \quad \text{and} \quad \phi^{(0)} = \mp\phi_0(\text{const.}) \quad \text{at} \quad z = \pm g(x). \tag{33}$$

In addition

$$\phi^{(0)} = E_0 z, E_l z \quad \text{and} \quad h^{(0)} = 0, -h_0(\text{const.}) \quad \text{at} \quad x = 0, l,$$

when the duct is joined at its ends to ducts of the types discussed previously. Here E_0, E_l are the values of $-(f')^{-1}d(f\,dh^{(0)}/dx)/dx$ coming from the adjacent ducts, and we have ensured continuity of pressure and electric potential across the joins. For the duct with parallel side walls these values are $-\phi_0/g(0)$ and $-\phi_0/g(l)$. Now $\phi^{(0)}$ and $h^{(0)}$ are determined. The constants ϕ_0 and h_0 (there is no analogue of the previous C_1 and C_2) can be calculated from the flux condition (2)

and the external resistance. Assuming that no account need be taken of the side layers, we find

$$h_0 = 2/(C+2\mathscr{R}f(0)) \quad \text{and} \quad \phi_0 = 2\mathscr{R}f(0)/(C+2\mathscr{R}f(0))$$

where C is the capacitance of the x, z region under the given boundary conditions on $h^{(0)}$.

Such a core solution can be matched with side layers, which are of the type discussed in §§2–5. Moreover core solutions which do not satisfy the conditions (33) cannot be matched: a non-zero tangential current requires a layer of the type considered in §6 and we saw that there is no such layer when $f' = 0$; while zero normal velocity is required automatically by the layer.

In fact the side layers are of particularly simple form. In equations (18), with tildes added, we have $v^{(0)} = j_x^{(\frac{1}{2})} = 0$ and $C_2 f^{-1}$ replaced by $-\partial h^{(0)}/\partial \tilde{x} - \partial \phi^{(0)}/\partial \tilde{z}$. Clearly $\beta = 1$ and the layer is that found by Hunt & Stewartson (1965) for fully developed flow, which corresponds to $g' \equiv 0$ here. It is the tangential core velocity which drives the layer; in fully developed flow this happens to be the axial velocity over the whole core section.

Part 1 pointed out that x, z lines of constant vertical separation of the duct walls play a special role in the core solution. When $f' \equiv 0$ all lines have this property, and the added flexibility of the core flow allows it to adapt to the side walls. For $f' \not\equiv 0$ no adaptation was necessary when $g' \equiv 0$, but for the general duct of §6 the lack of flexibility resulted in extreme side layers.

Note that a station where $g' = 0$ plays no special role. In fact the duct may have a whole portion where g' vanishes.

8. Generalizations and generalities

Three types of symmetric ducts have been considered, namely,

$$(a)\ g' \equiv 0, \quad (b)\ f', g' \not\equiv 0, \quad (c)\ f' \equiv 0.$$

Throughout we have assumed that f' does not change abruptly. When it does, a free shear layer extends across the duct at that section, signalled by an abrupt change in the core solution with x [see equations (10) with the definitions (13) and (31)]. However, the core current [even though $O(1)$] does not jump, so that the structure of such layers can be that found in part 1 on the inertialess approximation. Similar remarks apply to g' except for ducts of type (*c*): the potential core solution is infinitely smooth whatever its boundary conditions. With the addition of such free shear layers the theory is complete except, as noted earlier, near stations where $f' = 0$.

A general symmetric rectangular duct of variable area (with perfectly conducting side walls and insulating top and bottom) will be sectionally of one of the three types above. The appropriate part of our analysis still applies in each section, but the constants C_1 and C_2 (or h_0 and ϕ_0) are now determined by the flux condition and an overall external-circuit condition together with continuity conditions on h at each join. However, free shear layers will occur at each join even if f' and g' change continuously. This may be seen from the different character

of the side layers in the three cases: for type (*a*) there is no flux deficiency; for (*b*) part of the $O(1)$ flux is carried by the layers; and for (*c*) there is a flux deficiency. It is clear that there must be a free shear layer at every join to exchange fluid between the side layers and the core. (In fact it must be a particularly severe layer when (*b*) is involved since an $O(1)$ amount must be exchanged.)

The free layer at a join between (*a*) and (*b*) can be the inertialess kind described in part 1, since the core current does not jump. (Remember that the constants C_1 and C_2 are half the potential difference across the duct and a quarter of the flux down it.) But this is not true of the other two joins. In fact a join between (*b*) and (*c*) requires f' to vanish, which involves the infinities mentioned in §6. Similar remarks apply when a section of the duct is of constant area, i.e.

$$f' \equiv g' \equiv 0,$$

since this may be considered a special case of (*c*).

Free shear layers with a current jump deserve to be studied, but their analysis will be difficult for the reasons given in part 1. However, our present purpose is to find the overall flow, which requires no knowledge of these layers but merely faith in their existence. Here we have a contrast with the three-dimensional obstacle in a parallel-sided channel considered in part 1. While the precise structure of the layer was not required to determine the flow, certain gross properties of it were. Incidentally, the structure problem for such an obstacle placed in one of the present ducts is again difficult, since there is in general an $O(1)$ transverse current even when the side walls are on open circuit. The analysis in part 1 assumed the current-free state obtained in a duct of type (*c*) on open circuit. (Note that the free shear layers mentioned all stem from *geometrical* discontinuities, not *electrical*, as for example, found in Alty's (1966) experiments.)

We shall now summarize the main features of flow through the three types of ducts. In type (*a*) the two-dimensional solution of Hunt & Leibovich (1967) is valid everywhere except near the side walls, where matching layers are needed. The external circuit plays a very small role: a change in its resistance adjusts the mean pressure gradient, and hence transverse current, over the duct but does not affect the flow field. Deviations from the mean are determined at each cross-section by the height of the duct. An excess current across the duct at one section returns across sections where there is a deficiency, via the side walls.

The two profiles of the transverse velocity $w^{(\frac{1}{2})}$ illustrate the behaviour of the side layers. The 'slope' component W_1 gives a velocity away from the wall in a diverging duct. For an expansion between straight walls, its amplitude decreases like $f^{-\frac{3}{2}}$ while its scale increases like $f^{\frac{1}{2}}$: the fluid migrates away from the wall and gradients in the layer are eased. The 'curvature' component W_2 gives a velocity towards the wall when the convergence or divergence is increasing and away from the wall when there is decrease, even though in either case the layer is thinning or thickening respectively.

The core solution for type (*b*), is, of course, not two-dimensional, though the x and y velocities are still functions of x alone, as is the single, transverse component of current. Also the scale of the side layers is still $f^{\frac{1}{2}}$, but the transverse velocity $\tilde{w}^{(0)}$ is too complicated to draw worthwhile general conclusions. Instead

the flow may be characterized by the proportion of the total flux carried by the core; i.e. the $Q_c(x)$ of equation (32).

When there is no external load ($\mathscr{R} = 0$) we have

$$Q_c = 1 + (fg'/f'g);$$

there is an excess flux in the core for $g'/f' > 0$, i.e. a doubly converging or diverging duct (unimodal), and a deficient one for $g'/f' < 0$, i.e. a converging–diverging duct (bimodal). In the first case there is an equal backward flux in the side layers and in the second case an equal forward flux. The core flow is actually reversed when $g'/f' < -g/f$, i.e. when the relative change of the side walls is greater than that of the others in a bimodal duct.

An external load produces opposing volume fluxes. The core flux is increased in a bimodal duct and decreased in a unimodal one, by an amount which increases monotonically with $\mathscr{R}$. On open circuit ($\mathscr{R} = \infty$) we have

$$Q_c = 1 + \frac{fg'}{f'g}(1-\lambda) \quad \text{with} \quad \lambda(x;\infty) = \frac{f(x)\int_0^l d\xi/g(\xi)}{\int_0^l f(\xi)\,d\xi/g(\xi)}.$$

Clearly λ will be greater than 1 in parts of the duct and less than 1 elsewhere: in the former, an excess flux will be changed to a deficient and vice versa; in the latter, an excess or deficient flux will be reduced but not reversed.

As a simple example we consider exponential walls

$$f = A\,e^{-ax/l}, \quad g = e^{-bx/l},$$

for which

$$Q_c = (1 + (b/a)\,(1 - k e^{-ax/l}))\,(1 + O(M^{-\frac{1}{2}}, MN^{-1})),$$

where

$$k = rE(b)/[1 + rE(b-a)], \quad E(\alpha) = [e^{\alpha} - 1]/\alpha \quad \text{and} \quad r = \mathscr{R}Al.$$

(Because the flux in the boundary layer is $O(1)$, the higher-order terms are caused by higher-order magnetic–viscous effects in the core and boundary layers or by inertial effects which we have ignored throughout.) The parameters a and b represent the convergence of the y and z walls of the duct, while r is the resistance parameter. Note that $E(\alpha)$ is positive for all α. For all values of $a(\neq 0)$ and b, the constant k is finite and increases monotonically with r, in agreement with the general case above. The two extremes are

$$r = 0: \qquad k = 0,$$

$$r = \infty: \qquad k = E(b)/E(b-a) > 0.$$

When the side walls are shorted the core flux is constant along the duct, with an excess for a unimodal duct ($b/a > 0$) and a deficiency for a bimodal ($b/a < 0$) in accordance with the general theory. When the side walls are on open circuit these results are reversed over the part

$$\left(\frac{\log k}{a}\right) l < x < l \quad \text{for} \quad a < 0 \tag{34a}$$

and the part

$$0 < x < \left(\frac{\log k}{a}\right) l \quad \text{for} \quad a > 0, \tag{34b}$$

since k lies between 1 and e^a for all a. These are the parts of the duct referred to in the general discussion above.

The progress of the change from excess to deficiency, or vice versa, as the resistance increases can be readily seen in two special cases of our example. We have

$$k = \frac{r}{1+r} E(a) \quad \text{when} \quad a = b,$$

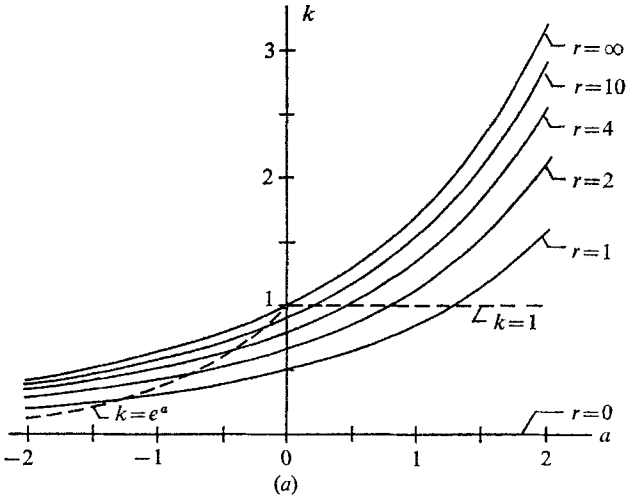

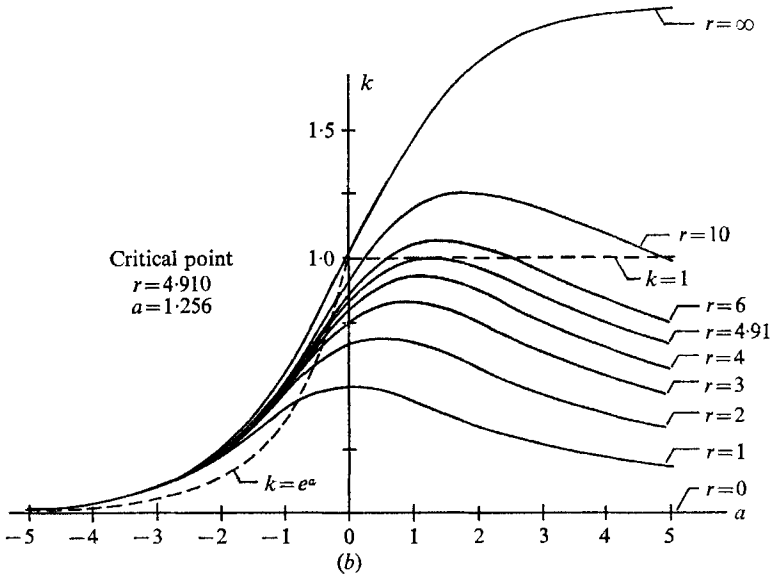

FIGURE 7. Proportion of flux through core for exponential divergences: k versus a. (*a*) Unimodal duct $a = b$. (*b*) Bimodal duct $a = -b$.

and figure 7 (*a*) gives graphs of k versus a for various values of r as well as the curve

$$k = \begin{cases} e^a & \text{for} \quad a < 0, \\ 1 & \text{for} \quad a > 0. \end{cases} \tag{35}$$

For points below this curve there is no reversal. So for any given a there is a minimum r which will change the core flux; and as r increases from its minimum the region of the duct affected (34*a* or *b*) spreads from the exit or entrance. As $|a|$ increases from zero to infinity, the minimum decreases from infinity to zero.

In the second case we have

$$k = \frac{rE(-a)}{1+rE(-2a)} \quad \text{when} \quad a = -b$$

and figure 7 (*b*) gives the new graphs of k versus a for various values of r as well as the curve (35). Again there is a minimum r for each a and the affected region spreads as before. The minimum still increases from zero to infinity as a increases from $-\infty$ to 0, but now as a increases from 0 to ∞ it passes from infinity to its own minimum (4·910 for $a = 1{\cdot}256$) and back to infinity again. When the y walls are converging (and the z walls diverging) in such a bimodal duct, there is a minimum $r = 4{\cdot}910$ below which there can never be a reversal of the core-flux deficiency which prevails for short-circuited side walls.

There is little to say about ducts of type (*c*), since the side layers have been described in detail by Hunt & Stewartson. However, two remarks can be made about the core flow, and indeed in essence could have been made by them. [In their case $h = -h_0 x/l$, $\phi = -\phi_0 z$ and $C = 2/l$.] When the duct is shorted ($\mathscr{R} = 0$), the pressure difference $2N/C$ drives the fluid with unit velocity, thereby inducing a unit transverse current which moves freely through the external circuit. When the duct is on open circuit ($\mathscr{R} = \infty$), a potential difference of 2 has built up across the duct to cancel the induced electric field of the fluid moving down the duct with unit velocity, and there is no pressure drop (to $O(N)$). [Similar but more complicated remarks can be made about ducts of types (*a*) and (*b*).]

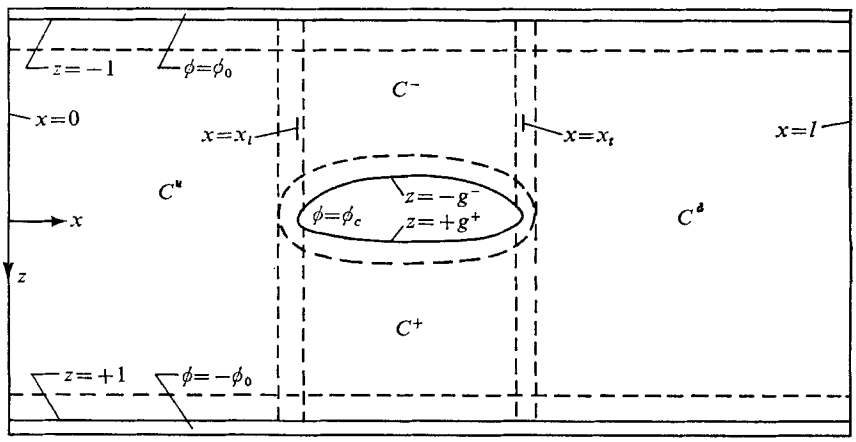

FIGURE 8. Duct with non-symmetric cylindrical obstacle placed parallel to magnetic field: y section showing core regions.

The analysis is easily extended to non-symmetric ducts. The possibilities then multiply to the point where it does not seem worth while to catalogue them. Instead we shall illustrate their *ad hoc* treatment with the example of a perfectly conducting cylinder

$$z = \pm g^{\pm}(x), \quad 0 < x_l \leqslant x \leqslant x_t < l$$

placed in the duct of figure 1. The various flow regions are indicated in figure 8.

Upstream and downstream of the cylinder, the duct is of type (*a*), so that, in the core region C^u, $h^{(0)}$ is given by equation (13) with

$$C_1^u = \phi_0, \quad C_2^u = f(0),$$

where $\mp\phi_0$ are the potentials of the walls $z = \pm 1$. Similarly in C^d

$$h^{(0)} = h^{(0)}(x_t) + C_1^d(x - x_t) - C_2^d \int_{x_t}^{x} f^{-1} dx, \tag{36}$$

where

$$C_1^d = \phi_0, \quad C_2^d = f(0)$$

and $h^{(0)}(x_t)$ will be determined later. In the core regions $C^{\pm}$ the arguments leading to the results (31) show that

$$h^{(0)} = h^{(0)}(x_l) + 2C_1^{\pm} \int_{x_l}^{x} \frac{dx}{1 - g^{\pm}} - 2C_2^{\pm} \int_{x_l}^{x} \frac{dx}{f(1 - g^{\pm})}, \tag{37}$$

where $h^{(0)}(x_l)$ is the value obtained in C^u. If ϕ_c is the potential of the cylinder and $Q^{\pm}$ are the total fluxes between it and $z = \pm 1$,

$$C_1^{\pm} = \tfrac{1}{2}\phi_0 \pm \tfrac{1}{2}\phi_c, \quad C_2^{\pm} = \tfrac{1}{4}Q^{\pm}.$$

[The corresponding formulas for $\psi^{(0)}$ will not be needed.] Since

$$Q^+ + Q^- = 4f(0)$$

there are just three constants (ϕ_0, ϕ_c and Q^+ say) to be determined.

One condition for these constants is that the change in pressure (i.e. h) should be the same above and below the cylinder: the values of h at $x = x_t$ calculated from the two formulas (37) are to be set equal. After the constants have been determined this common value is to be used in the formula (36). The remaining two conditions come from the external circuit, which quite generally may be considered as the connection of the two walls and the cylinder to each other in pairs through three resistances. The total currents entering the two walls and the cylinder (i.e. the nodes of the external circuit) can be calculated in terms of the three constants from the $h^{(0)}$ formulas above. [Three conditions are then obtained but one more unknown, the loop current, is introduced.]

Instead of writing down these conditions in general we take the special case of shorted walls and cylinder (all resistances zero). Then

$$\phi_0 = \phi_c = 0 \quad \text{and} \quad Q^+ \int_{x_l}^{x_t} \frac{dx}{f(1 - g^+)} = Q^- \int_{x_l}^{x_t} \frac{dx}{f(1 - g^-)}.$$

Limitations of the inertialess approximation. We have assumed that the applied magnetic field is sufficiently strong for inertial effects to be negligible. The

accuracy of this inertialess approximation in any physical situation depends on the relative sizes of N and M. Eventually inertia must be taken into account, and the expansion solution must include terms which involve both N and M. The curl of equation (4*a*), together with equations (4*b*, *d*), yields an equation involving only the velocity,

$$\partial^2\mathbf{v}/\partial y^2 - M^{-2}\nabla^4\mathbf{v} = N^{-1}\nabla(\nabla.[(\mathbf{v}.\nabla)\mathbf{v}]) - N^{-1}\nabla^2[(\mathbf{v}.\nabla)\mathbf{v}].$$

For ducts of types (*a*) and (*c*), where one pair of walls is parallel, the appropriate inertialess expansion (6) is a power series in $M^{-\frac{1}{2}}$ beginning with an $O(1)$ term, while, for ducts of type (*b*) where both pairs of walls diverge, the first term in the expansion is $O(M^{\frac{1}{2}})$. In both expansions, the first term involving N is created by the inertial error of the leading inertialess term in the side-wall boundary layers, but it has a different magnitude for the two expansions.

In ducts of types (*a*) and (*c*), the largest inertial error involves terms such as

$$N^{-1}\partial^2(u\,\partial u/\partial x)/\partial z^2 = MN^{-1}\partial^2(u^{(0)}\partial u^{(0)}/\partial x)/\partial\zeta^2$$

in the side layers. The first inertial term in the expansion (6) is $O(MN^{-1})$ and is negligible compared to our inertialess solution $u^{(0)}$, if

$$MN^{-1} \ll 1 \rightarrow N \gg R \quad \text{or} \quad M \gg R.$$

In ducts of type (*b*), the corresponding inertial error in the side layers is

$$N^{-1}\partial^2(\tilde{u}\,\partial\tilde{u}/\partial\tilde{x})/\partial\tilde{z}^2 = M^2N^{-1}\partial^2(\tilde{u}^{(-\frac{1}{2})}\partial\tilde{u}^{(-\frac{1}{2})}/\partial\tilde{x})/\partial\zeta^2.$$

The resulting $O(M^2N^{-1})$ inertia term in the second type of expansion is negligible compared to $M^{\frac{1}{2}}u^{(-\frac{1}{2})}$ if

$$M^2N^{-1} \ll M^{\frac{1}{2}} \rightarrow N \gg R^3 \quad \text{or} \quad M^{\frac{1}{2}} \gg R.$$

This is the same restriction required for the theory of part 1, which dealt with free shear layers involving $O(M^{\frac{1}{2}})$ velocities. The appropriate criterion for the inertialess approximation in each type of duct should be added to the general assumptions (5).

This research was supported partly by the U.S. Army Research Office–Durham and partly by the National Science Foundation under Grant GF 8711.

REFERENCES

ALTY, C. J. N. 1966 Magnetohydrodynamic duct flow in a transverse magnetic field of arbitrary orientation. Ph.D. Thesis, Cambridge University.

CARLEMAN, T. 1922 Über die Abelsche Integralgleichung mit konstanten Integrationsgrengen. *Math. Z.* **15**, 111–120.

CHIANG, D. & LUNDGREN, T. 1967 Magnetohydrodynamic flow in a rectangular duct with perfectly conducting electrodes. *Z. angew. Math. Phys.* **18**, 92–104.

HUNT, J. C. R. 1965 Magnetohydrodynamic flow in rectangular ducts. *J. Fluid Mech.* **21**, 577–590.

HUNT, J. C. R. 1970 The resistance of a blunt body in a strong transverse magnetic field. *Magnitnaya Gidrodinamika*, **6**, no. 1, 35–38. (In Russian translation from author.)

HUNT, J. C. R. & LEIBOVICH, S. 1967 Magnetohydrodynamic flow in channels of variable cross-section with strong transverse magnetic field. *J. Fluid Mech.* **28**, 241–260.

HUNT, J. C. R. & LUDFORD, G. S. S. 1968 Three-dimensional MHD duct flows with strong transverse magnetic fields. Part 1. Obstacles in a constant area channel. *J. Fluid Mech.* **33**, 693–714.

HUNT, J. C. R. & STEWARTSON, K. 1965 Magnetohydrodynamic flow in rectangular ducts II. *J. Fluid Mech.* **23**, 563–581.

KALIS, KH. E., SLYUSAREV, N. M., TSINOBER, A. B. & SHTERN, A. G. 1966 Resistance of bluff bodies at high Stuart numbers. *Magnitnaya Gidrodinamika*, **2**, 152–153.

KULIKOVSKII, A. G. 1968 Steady, slow flows of conducting fluid at large Hartmann number. *Mekh. Zhidkosti i Gaza*, no. 2, 3–10.

MOFFATT, H. K. 1964 Electrically driven steady flows in magnetohydrodynamics. *Proc. 11th Internat. Congr. of Appl. Mech. (Munich)*, p. 946–935.

WALKER, J. S. 1970 Three-dimensional magnetohydrodynamic flow in diverging, rectangular ducts under strong transverse magnetic fields. Ph.D. thesis, Cornell University.